Appl. Phys. B 69, 473–476 (1999) / Digital Object Identifier (DOI) 10.1007/s003409900085

Applied Physics B
Lasers
and Optics

Photoacoustic method for orientation and optical characterization of nonlinear crystals

J.O. Tocho[1,*], **G.M. Bilmes**[1,**], **H.F. Ranea Sandoval**[2,*]

[1] Universidad Nacional de La Plata and Centro de Investigaciones Ópticas (CONICET, CIC), CC. 124, 1900-La Plata, Argentina
(Fax: +54-221/471-2771, E-mail: JorgeT@ciop.unlp.edu.ar; gbilmes@volta.ing.unlp.edu.ar)
[2] Instituto de Física "Arroyo Seco" – FCE – Universidad Nacional del Centro de la Provincia de Buenos Aires, Pinto 399, 7000 Tandil, Argentina
(E-mail: hranea@ifas.exa.unicen.edu.ar)

Received: 27 July 1998/Revised version: 19 March 1999/Published online: 19 August 1999

Abstract. Second-harmonic conversion of the 532-nm pulsed output of a doubled Nd:YAG laser in KDP was characterized by analyzing the changes in the acoustic signals generated in the crystal at different orientation conditions and for several incident fluences. Using a piezoelectric transducer, phase-matching condition was determined by maximizing the amplitude of the acoustic signals detected. The angular orientation for optimum harmonic efficiency was obtained with the same precision compared with the conventional optical procedure. The origin of the photoacoustic signals is the relaxed energy following the absorption of 266-nm photons. To determine the mechanisms of the 266-nm absorption processes, we also performed experiments under direct illumination with the 266-nm emission of the quadrupled Nd:YAG laser. A combination of a linear and nonlinear process occurs. Direct absorption by KDP as well as the participation of transient defects produced in the material were analyzed.

PACS: 42.65.Ky; 43.85.+f; 78.20.Dj

Laser generation of acoustic waves in different media has been extensively studied for both weakly and strongly absorbing materials. In the general case, the amplitude and shape of the generated photoacoustic signal are dependent on the optical and thermoelastic properties of the sample, on the spatial and temporal properties of the laser pulse, and on the experimental geometry. Then, any change in one of these parameters produces changes in the generated acoustic signals.

Recently it was shown how the acoustic waves induced by laser pulses can be used to characterize a pulsed dye laser, to align different components of it, as well as to measure laser beam diameters and relative positions in order to achieve beam overlap in different experiments [1, 2].

This procedure can be applied in optical experiments that use nonlinear crystals as, for example, frequency conversion. As is very well known, maximum conversion efficiency to harmonics requires an orientation procedure, that sometimes is somewhat cumbersome especially in the near-IR region where detectors have low efficiency and speed.

The main idea of the method proposed here is based on the fact that some of the laser energy deposited on a nonlinear crystal is converted into heat, generating an acoustic wave whose characteristics are dependent among others, on the orientation of the crystal. Thus, any change in the amount of heat generated in the sample produces changes in the acoustic signals, providing a sensitive and real-time method for monitoring nonlinear conversion, and for the characterization of crystal properties. Second-harmonic generation (SHG) was selected to show the possibilities of the developed method, but results can be extended to other situations.

In this work we show how photoacoustics can be used as a reliable and precise tool to properly orient a KDP crystal, in order to achieve the phase-matching condition for SHG.

Additionally, the absorption mechanism of the 266-nm photons in this material was studied for pumping intensities up to 7 MW/cm^2.

1 Experimental

The second-harmonic (532 nm) output of a Nd:YAG laser was doubled in KDP in an experimental arrangement displayed in Fig. 1. The sample crystal, a cube of 1 cm side was oriented near the phase-matching condition; to do this, a three-circle mount was used. A piezoelectric transducer (PZT) was glued to one of the crystal faces and the acoustic signal recorded in a digital storage oscilloscope without any further amplification. Pulse incident intensities of the 532-nm input ($E\omega$), and the 266-nm output ($E2\omega$) were also measured using two pyroelectric detectors (P). The incident beam was limited by a 1-mm-diameter iris and its density was changed with a double-wedged attenuator.

The photoacoustic signal (PAS) was taken as the peak-to-peak amplitude of the first cycle of the ringing acoustic wave as shown in Fig. 2. The noise produced mainly by the Q-switch firing is shown in part (a) where the laser was

* Member of the Carrera del Investigador Científico CONICET
** Member of the Carrera del Investigador Científico CIC-BA.

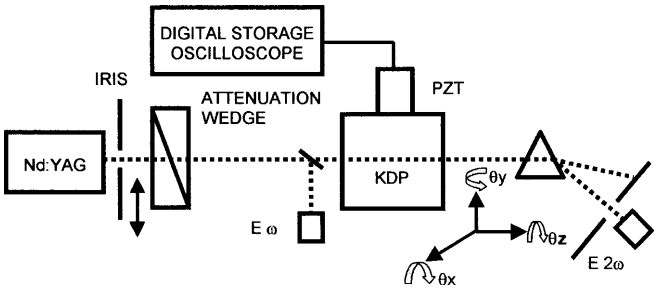

Fig. 1. Block diagram of the experiment for the characterization of the SHG in KDP using the photoacoustic method described. The 266-nm further absorption experiment has a similar layout

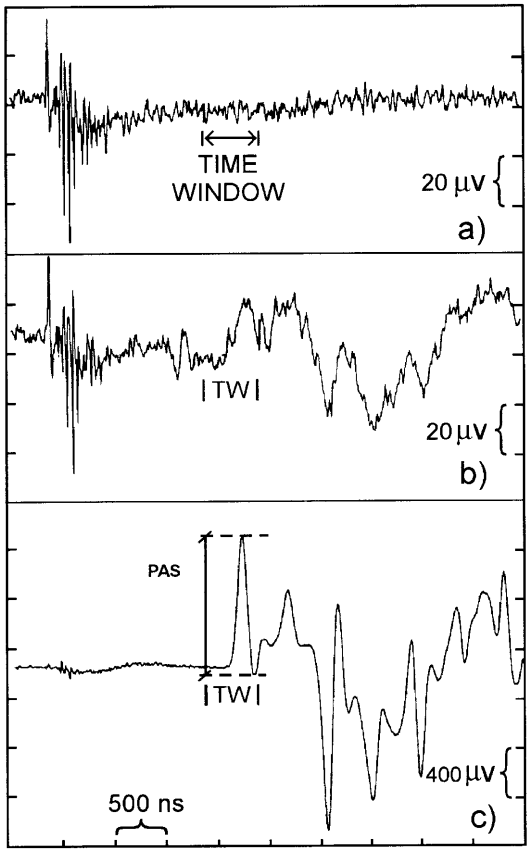

Fig. 2a–c. Piezoelectric transducer signals. **a** Noise produced by laser firing when the beam is blocked before the crystal. **b** Photoacoustic signal obtained for crystal orientation far from phase-matching condition. **c** Photoacoustic signal obtained for crystal at phase-matching condition. Note the change in vertical scale. PAS is defined as the peak-to-peak amplitude of the photoacoustic signal in the selected time-window

blocked before it reaches the crystal; acoustic signal produced far from the phase-matching condition is shown in part (b); and the signal generated at the phase-matching orientation is shown in part (c).

2 Results and discussion

The sensitivity of the alignment procedure can be observed in Fig. 3 where PAS and the intensity of the 266-nm generated pulses, for a fixed 532-nm input and optimum θ_z angle, were

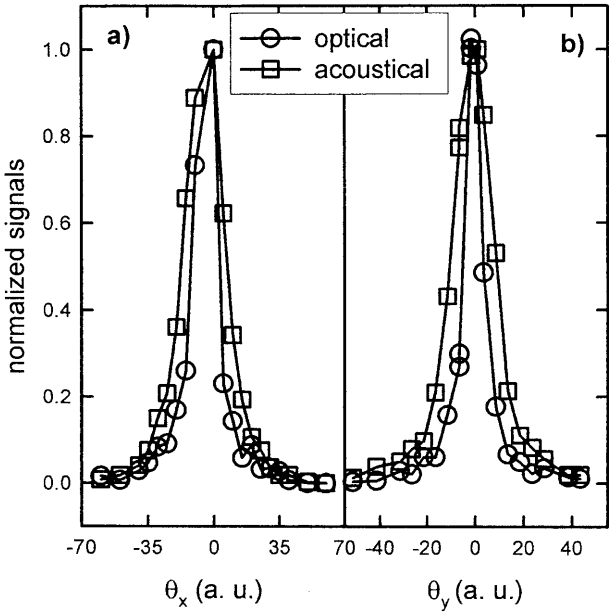

Fig. 3. Output intensity at 266 nm and PAS vs. the angles of orientation of the KDP crystal as indicated in Fig. 1

plotted for different values of the other orientation angles, noted as θ_x and θ_y. The maximization of the PAS allowed the orientation of the crystal to the optimum experimental phase-matching conditions with the same precision as the conventional optical measurements. As can be seen, the acoustic curve is slightly wider than the optical one. This fact is an advantage of the photoacoustic method, because the phase-matching condition can be reached easily even in the cases in which the orientation procedure starts from severe misalignment.

To search for the physical origin of the PAS we have studied its dependence with the incident intensity on the crystal at the phase-matching condition. Figure 4 shows the PAS

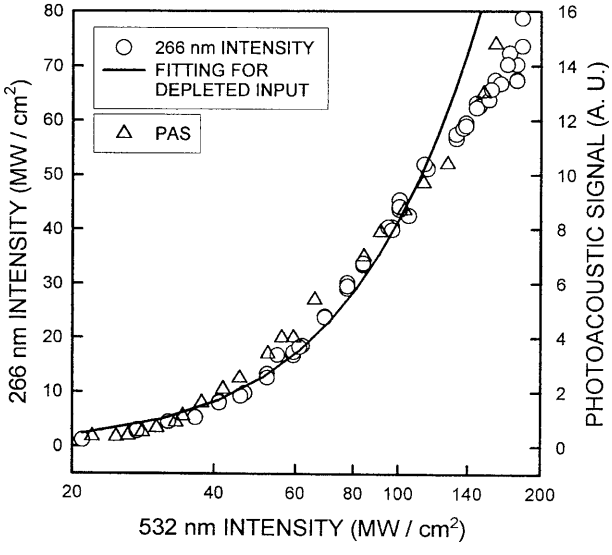

Fig. 4. Optical output intensity at 266 nm and PAS, at phase-matching conditions, vs. 532-nm incident intensity. The *solid line* corresponds to (1) applied to KDP

and the converted 266-nm intensity as a function of the incident intensity at 532 nm. As can be seen, there is a good correlation between both measurements.

Figure 4 also shows how the results of these experiments can be fitted with a standard expression for SHG with depleted input, as it was evident in our case [3],

$$I_{266\ \mathrm{nm}} = I_{532\ \mathrm{nm}} \times \tanh^2\left[\left(\frac{I_{532\ \mathrm{nm}}}{I_{\mathrm{sat}}}\right) \times L\right], \qquad (1)$$

where $I_{\mathrm{sat}} = 1.7 \times 10^8\ \mathrm{W/cm^2}$, was evaluated using literature values for KDP [4].

Using the facts that the absorbed energy at 532 nm is extremely low [4], the acoustic signal at a fixed 532-nm input fluence is dependent of the orientation of the crystal (Fig. 3), and the results of Fig. 4, we conclude that the origin of the PAS is the energy converted to heat following the absorption of 266-nm photons.

In order to determine how the crystal absorbs the 266-nm photons, the KDP sample was pumped directly with pulses of 266 nm, from the frequency-quadrupled output of the Nd:YAG laser. Figure 5 displays the amplitude of the PAS recorded as a function of the 266-nm intensity of the pulse impinging on the crystal.

The behavior of the experimental data is typical of combined linear and nonlinear processes.

In a first attempt to explain the obtained results, PAS was assumed to be proportional to the non-radiative fast relaxation following a linear, one photon, and a nonlinear, two-photon absorption process at 266 nm. In this case, PAS can be written as [5],

$$\mathrm{PAS} = K I_{266\ \mathrm{nm}}\left[I - \frac{\exp(-\alpha L)}{I + \frac{\beta}{\alpha} I_{266\ \mathrm{nm}}[1 - \exp(-\alpha L)]}\right], \qquad (2)$$

where all the characteristics of the PZT and the particular mounting are dumped in K, and α and β are the coefficients for linear and nonlinear absorption for KDP at 266 nm, respectively. Inspection of (2) shows that the nonlinear behavior becomes important as I_{266} is greater than the value α/β. From published values, α and β at 266 nm range between 0.02–0.04 $\mathrm{cm^{-1}}$ and 0.03–0.06 cm/GW respectively [4–6], and the critical value for I_{266} is expected to be at least over 330 $\mathrm{MW/cm^2}$. This is not the case of our experimental data where the linear behavior is broken above 2 $\mathrm{MW/cm^2}$. The way to force (2) to fit our data is by assuming very low values for the linear absorption coefficient, as is shown in Fig. 5, or alternatively, by using quite large values for the nonlinear absorption coefficient.

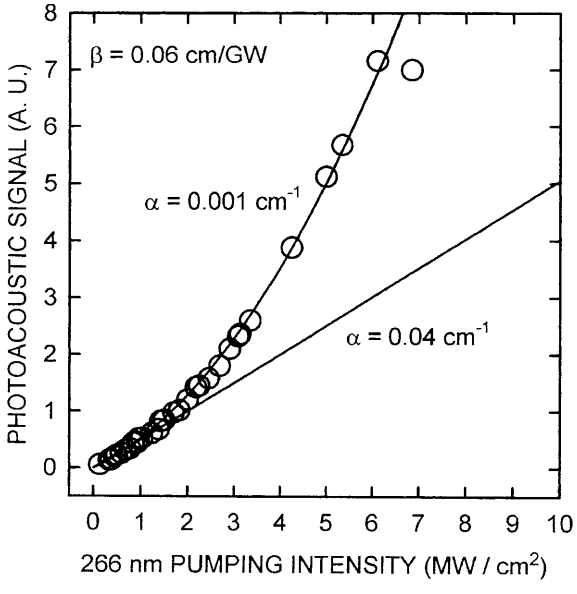

Fig. 5. PAS vs. the intensity of the 266-nm incident radiation. *Solid lines* correspond to (2) for different values of linear absorption; K was selected to adjust the experimental points for low intensity ($< 2\ \mathrm{MW/cm^2}$)

A more realistic way to explain the results of Fig. 5 is to assume the presence of a transient species absorbing at 266 nm. The production of transient color centres in KDP crystal after a two-photon coherent process at 266 nm, was previously demonstrated [4]. These defects have strong absorption in the visible and UV, including at 266 nm. Then, further non-radiative relaxation of the excited transient, leads to an additional source of heat that can explain at least qualitatively, the nonlinear behavior of the experimental data of Fig. 5.

Following the considerations of Marshall et al. [4], the color centres formed by absorption of 266 nm are bleached at higher intensities of the same radiation. As result of this, the density of color centres has a quadratic dependence with pumping intensity that changes to linear at higher intensities. This fact can explain the difference in angular width of the optical and PAS data of Fig. 3 since the rate of heat production, responsible for the acoustic signal, is reduced near the center (phase-matching condition) with respect to the wings.

3 Conclusions

We developed a new real-time method to achieve the phase-matching condition for SHG in nonlinear crystals. Optimum conversion can be reached in KDP by monitoring and maximizing the acoustic signal, generated in the crystal during laser irradiation, as a function of the orientation of the crystal.

The acoustic signals produced when KDP is doubling a 532-nm input are due to a rapid deactivation process following the 266-nm photon absorption.

The amount of heat produced after a direct linear and nonlinear absorption of 266-nm photons is not enough to explain the experimental results obtained, at least with the reported values for the absorption coefficients.

Additional absorption of 266-nm photons by a transient species generated in the crystal can contribute to the generation of the acoustic signals. Reported color centres, formed in KDP by a two-photon process, have enough absorption at 266 nm to produce the enhancement observed in the acoustic signal. Further study is necessary in this direction to determine effectively the participation of color centres in the generation of the acoustic signal, and to evaluate quantitatively its effect at fluences of the order of 2 $\mathrm{MW/cm^2}$.

Acknowledgements. This work is partially supported by CONICET, CICBA, UNLP, and UNCPBA.

References

1. M. Villagrán-Muniz, C. García Segundo, H.F. Ranea-Sandoval, G.M. Bilmes: Rev. Sci. Instrum. **66**, 3500 (1995)
2. M. Villagrán-Muniz, C. García-Segundo, H.F. Ranea-Sandoval, C. Gogorza, G.M. Bilmes: Appl. Phys. B **61**, 361 (1995)
3. A. Yariv: *Quantum Electronics*, 2nd edn. (Wiley, New York 1975) p. 430
4. C.D. Marshall, S.A. Paine, M.A. Henesian, J.A. Speth, H.T. Powell: J. Opt. Soc. Am. B **11**, 774 (1994)
5. J. Reintjes, R.C. Eckardt: IEEE J. Quantum Electron **QE-13**, 791 (1977)
6. G.F. Wang, G.Y. Ma, G.P. Chen, Z.D. Xu, Y.S. Wang, G.Y. Zhang, X.Q. Li: Phys. Lett. A **29**, 166(5-6), 433 (1992)